Alkylidyne(carbaborane) Complexes of the Group 6 Metals. Part 6.[1] *exo-nido*-Tungstacarbaborane Compounds‡

Stephen A. Brew, John C. Jeffery, Mark D. Mortimer and F. Gordon A. Stone *†
School of Chemistry, The University, Bristol BS8 1TS, UK

Protonation of mixtures of $[NEt_4][Mo(\equiv CC_6H_4Me\text{-}4)(CO)\{P(OMe)_3\}(\eta^5\text{-}C_2B_9H_9Me_2)]$ and $[W(\equiv CR)(CO)_2(\eta\text{-}C_5R'_5)]$ ($R = C_6H_4Me\text{-}4$ or Me, $R' = H$; $R = C_6H_4Me\text{-}4$, $R' = Me$) with $HBF_4{\cdot}Et_2O$ in CH_2Cl_2 at −78 °C affords the mononuclear tungsten complexes $[\mathit{exo\text{-}nido}\text{-}9,10\text{-}\{W(CO)_2(\eta\text{-}C_5R'_5)\}\text{-}9,10\text{-}(\mu\text{-}H)_2\text{-}7,8\text{-}C_2B_9H_8\text{-}7,8\text{-}Me_2]$. An X-ray diffraction study ($R' = Me$) reveals a structure which may be regarded formally as an ion pair, with a $[\mathit{nido}\text{-}7,8\text{-}C_2B_9H_{10}Me_2]^-$ anion co-ordinated to a $[W(CO)_2(\eta\text{-}C_5Me_5)]^+$ cation by two exopolyhedral three-centre two-electron B–H→W bonds. The boron atoms forming these linkages lie in the open pentagonal $\overline{\mathrm{CCBBB}}$ face of the cage and are adjacent. The remaining B–B connectivity in this face is bridged by a hydrogen atom. Data from ^{11}B–^1H and ^{11}B–^{11}B correlation NMR spectroscopy of the compound are reported and are fully in agreement with the structure. Treatment of an equimolar mixture of $[NEt_4][W(\equiv CC_6H_4Me\text{-}4)(CO)_2(\eta^5\text{-}C_2B_9H_9Me_2)]$ and $[W(\equiv CC_6H_4Me\text{-}4)(CO)_2(\eta\text{-}C_5H_5)]$ in CH_2Cl_2 at −78 °C with $HBF_4{\cdot}Et_2O$ affords the dimetal complex $[W_2(\mu\text{-}CC_6H_4Me\text{-}4)(CO)_3(\eta^5\text{-}C_2B_9H_9Me_2)(\eta\text{-}C_5H_5)]$. In contrast, if the salt $[PPh_4][W(\equiv CC_6H_4Me\text{-}4)(CO)_2(\eta^5\text{-}C_2B_9H_{11})]$ is employed in a similar reaction, carried out at room temperature, the product obtained, as shown by NMR spectroscopy, exists in solution as an equilibrium mixture (*ca.* 10:1) of two isomers, the major species being highly fluxional. Crystals of the latter were obtained from solution, and an X-ray diffraction analysis revealed the complex to be $[\mathit{exo\text{-}nido}\text{-}9,11\text{-}(CH_2C_6H_4Me\text{-}4)_2\text{-}5,10\text{-}\{W(CO)_2(\eta\text{-}C_5H_5)\}\text{-}5,10\text{-}(\mu\text{-}H)_2\text{-}7,8\text{-}C_2B_9H_8]$. In this unusual structure the two boron atoms adjacent to the carbons in the open $\overline{\mathrm{CC}\mathit{B}\mathrm{B}\mathit{B}}$ face of the *nido*-C_2B_9 anion carry $CH_2C_6H_4Me\text{-}4$ substituents. The remaining boron atom forms a B–H→W bridge to the exopolyhedral $[W(CO)_2(\eta\text{-}C_5H_5)]^+$ fragment, which is also attached to the cage through a second B–H→W linkage, involving a boron atom in the pentagonal boron layer below the face. The NMR data suggest that the minor isomer existing in solution is a *closo*-icosahedral species $[WH(CO)_2\{\eta^3\text{-}7,8\text{-}C_2B_9H_9\text{-}9,11\text{-}(CH_2C_6H_4Me\text{-}4)_2\}(\eta\text{-}C_5H_5)]$.

Treatment of the anionic complexes $[W(\equiv CR)(CO)_2(\eta^5\text{-}7,8\text{-}C_2B_9H_9Me_2)]^-$ (R = alkyl or aryl) in CH_2Cl_2 at *ca.* −78 °C with $HBF_4{\cdot}Et_2O$ in the presence of donor molecules (CO, $CNBu^t$, tertiary or secondary phosphines, alkynes, *etc.*) affords a variety of mononuclear tungsten compounds with novel structures.[1,2] In many of the products the metal atom is η^5 ligated by a *nido*-$C_2B_9H_8(CH_2R)Me_2$ icosahedral fragment. The CH_2R groups in the latter evidently arise *via* insertion of an initially formed tungsten-bonded alkylidene moiety into a B–H bond lying in the open pentagonal $\overline{\mathrm{CCBBB}}$ face of the carbaborane cage. Invariably the boron atom carrying the CH_2R substituent is in the β site with respect to the two carbon atoms.

Similar experiments involving treatment of the species $[M(\equiv CR)(CO)_2(\eta^5\text{-}7,8\text{-}C_2B_9H_9Me_2)]^-$ (M = Mo or W) with $HBF_4{\cdot}Et_2O$ in the presence of the reagents $[M(\equiv CR)(CO)_2(\eta\text{-}C_5H_5)]$ afford dimetal compounds. However, the nature of the latter depends critically on several factors, including reaction temperatures and the character of the substituents R attached to the alkylidyne carbon atoms.[3] Thus treatment of the molybdenum salt **1a** in CH_2Cl_2 at −78 °C with $HBF_4{\cdot}Et_2O$ in the presence of $[W(\equiv CMe)(CO)_2(\eta\text{-}C_5H_5)]$ affords $[MoW(\mu\text{-}CMe)(CO)_3\{\eta^5\text{-}C_2B_9H_8(CH_2C_6H_4Me\text{-}4)Me_2\}(\eta\text{-}C_5H_5)]$ **2a**.[3a] Similarly, the complex $[W_2(\mu\text{-}CMe)(CO)_3\{\eta^5\text{-}C_2B_9H_8(CH_2C_6H_4Me\text{-}4)Me_2\}(\eta\text{-}C_5H_5)]$ **2b** is formed by adding $HBF_4{\cdot}Et_2O$ to a mixture of **1b** and $[W(\equiv CMe)(CO)_2(\eta\text{-}C_5H_5)]$ in CH_2Cl_2. In contrast, addition of $HBF_4{\cdot}Et_2O$ to equimolar quantities of **1b** and $[W(\equiv CC_6H_4Me\text{-}4)(CO)_2(\eta\text{-}C_5H_5)]$ gives the compound $[W_2(\mu\text{-}CC_6H_4Me\text{-}4)(CO)_3(\eta^5\text{-}C_2B_9H_9Me_2)(\eta\text{-}C_5H_5)]$ **3a**, resulting from loss of a $C(H)C_6H_4Me\text{-}4$ fragment. Interestingly, treatment of a mixture of $[NEt_4][W(\equiv CC_6H_4Me\text{-}4)(CO)_2(\eta^6\text{-}7,9\text{-}C_2B_{10}H_{10}Me_2)]$ **4** and $[W(\equiv CC_6H_4Me\text{-}4)(CO)_2(\eta\text{-}C_5H_5)]$ with $HBF_4{\cdot}Et_2O$ affords $[W_2(\mu\text{-}CC_6H_4Me\text{-}4)(CO)_3(\eta^5\text{-}C_2B_9H_9Me_2)(\eta\text{-}C_5H_5)]$ **5a**. The latter forms *via* loss of both a $C(H)C_6H_4Me\text{-}4$ fragment and a BH vertex. Complex **5a** is an isomer of **3a**, having an $\eta^5\text{-}7,9\text{-}C_2B_9H_9Me_2$ ligated *nido* cage, as opposed to the $\eta^5\text{-}7,8\text{-}C_2B_9H_9Me_2$ arrangement present in **3a**. Moreover, **5a** is thermodynamically the more stable isomer, since it forms quantitatively when **3a** is heated in toluene.[3a] Related to the synthesis of **5a** are the preparation of $[W_2(\mu\text{-}CC_6H_4Me\text{-}4)(CO)_3(\eta^6\text{-}7,9\text{-}C_2B_{10}H_{10}Me_2)(\eta\text{-}C_5H_5)]$ **6a** from the reaction between the salt **4**, $[W(\equiv CMe)(CO)_2(\eta\text{-}C_5H_5)]$ and $HBF_4{\cdot}Et_2O$, and the formation of a mixture of the complexes $[MoW(\mu\text{-}CC_6H_4Me\text{-}4)(CO)_3(\eta^5\text{-}7,9\text{-}C_2B_9H_9Me_2)(\eta\text{-}C_5H_5)]$ **5b** and $[MoW(\mu\text{-}CC_6H_4Me\text{-}4)(CO)_3(\eta^6\text{-}7,9\text{-}C_2B_{10}H_{10}Me_2)(\eta\text{-}C_5H_5)]$ **6b** from a combination of the reagents **4**, $[Mo(\equiv CC_6H_4Me\text{-}4)(CO)_2(\eta\text{-}C_5H_5)]$ and $HBF_4{\cdot}Et_2O$.[3a]

The above results amply demonstrate the diverse nature of dimetal species obtained by treating the salts **1a**, **1b**, or **4** with $HBF_4{\cdot}Et_2O$ in the presence of the compounds $[M(\equiv CR)(CO)_2(\eta\text{-}C_5H_5)]$. In this paper we report studies on some related reactions. Unexpectedly, mononuclear tungsten products have been obtained, having $[W(CO)_2(\eta\text{-}C_5R'_5)]^+$ ($R' = H$ or Me) fragments bonded to $[\mathit{nido}\text{-}C_2B_9]^-$ cage anions *via* two three-centre two-electron (3c–2e) B–H→W linkages.

Results and Discussion

An equimolar mixture of the molybdenum salt **1c** and $[W(\equiv CC_6H_4Me\text{-}4)(CO)_2(\eta\text{-}C_5H_5)]$ in CH_2Cl_2 at −78 °C was

---

† *Present address:* Department of Chemistry, Baylor University, Waco, TX 76798-7348, USA.

‡ *Supplementary data available:* see Instructions for Authors, *J. Chem. Soc., Dalton Trans.*, 1992, Issue 1, pp. xx–xxv.

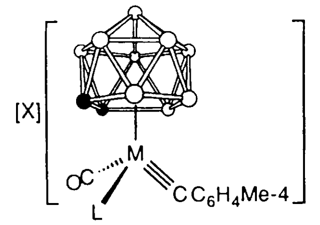

	X	M	L	●
1a	NEt$_4$	Mo	CO	CMe
1b	NEt$_4$	W	CO	CMe
1c	NEt$_4$	Mo	P(OMe)$_3$	CMe
1d	PPh$_4$	W	CO	CH

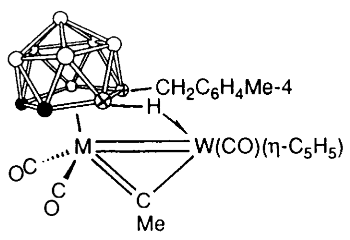

⊕ B

	M	●
2a	Mo	CMe
2b	W	CMe

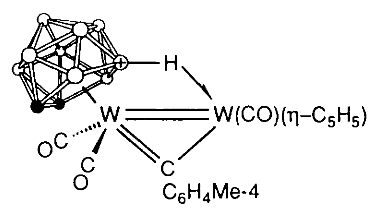

	●
3a	CMe
3b	CH

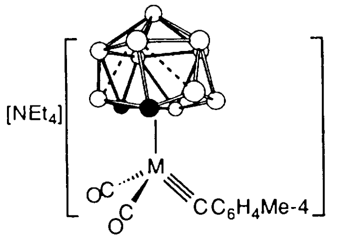

4

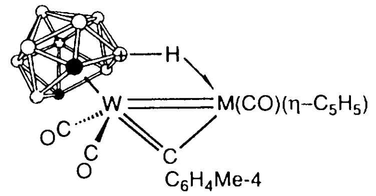

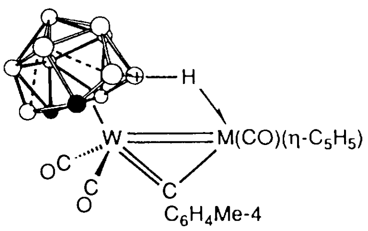

● CMe ○ BH ⊕ B

	M
5a	W
5b	Mo

	M
6a	W
6b	Mo

Table 1 Analytical[a] and physical data for the tungsten complexes

Compound[b]	Colour	Yield (%)	ν_{max}(CO)[c]/cm^{-1}	Analysis (%) C	Analysis (%) H
3b [W$_2$(μ-CR)(CO)$_3$(η^5-C$_2$B$_9$H$_{11}$)(η-C$_5$H$_5$)]	Green	89	[d]2007s, 1957s, 1934w(sh)	29.1 (28.7)	3.7 (3.1)
7a [*exo-nido*-9,10-{W(CO)$_2$(η-C$_5$H$_5$)}-9,10-(μ-H)$_2$-7,8-C$_2$B$_9$H$_8$-7,8-Me$_2$]	Deep blue	11	1974s, 1894s	29.2 (28.3)	4.6 (4.5)
7b [*exo-nido*-9,10-{W(CO)$_2$(η-C$_5$Me$_5$)}-9,10-(μ-H)$_2$-7,8-C$_2$B$_9$H$_8$-7,8-Me$_2$]	Purple	14	1956s, 1874s	36.4 (35.8)	5.9 (5.8)
9a [*exo-nido*-9,11-(CH$_2$R)$_2$-5,10-{W(CO)$_2$(η-C$_5$H$_5$)}-5,10-(μ-H)$_2$-7,8-C$_2$B$_9$H$_8$]	Red	53	[e]2030w, 1985m, 1950m, 1926s, 1874m, 1840m	46.0 (46.4)	5.2 (5.1)

[a] Calculated values are given in parentheses. [b] R = C$_6$H$_4$Me-4. [c] Measured in hexane unless otherwise stated. All compounds show a broad band at *ca.* 2570 cm^{-1} due to B–H absorptions. [d] In CH$_2$Cl$_2$. [e] Mixture of isomers, see text.

treated with an equivalent of HBF$_4$·Et$_2$O in the expectation of forming a molybdenum–tungsten dimetal complex with a structure similar to those of compounds **2** or **3a**. After column chromatography of the reaction mixture a blue crystalline compound **7a** was isolated in relatively low yield, partly due to its decomposition during the purification procedures. A similar reaction employing [W(≡CMe)(CO)$_2$(η-C$_5$H$_5$)] instead of [W(≡CC$_6$H$_4$Me-4)(CO)$_2$(η-C$_5$H$_5$)] afforded the same blue compound, and it was apparent from microanalytical and spectroscopic data (Tables 1 and 2) that **7a** was a mononuclear rather than a dinuclear metal species.

The puzzling nature of the results was clarified following a study of the reaction between **1c**, [W(≡CC$_6$H$_4$Me-4)(CO)$_2$(η-C$_5$Me$_5$)] and HBF$_4$·Et$_2$O in CH$_2$Cl$_2$ at −78 °C. The product isolated was the complex [*exo-nido*-9,10-{W(CO)$_2$(η-C$_5$Me$_5$)}-9,10-(μ-H)$_2$-7,8-C$_2$B$_9$H$_8$-7,8-Me$_2$] **7b**, the structure of which was established by detailed NMR studies, including ^{11}B–^{11}B and ^{11}B–^{1}H correlation spectroscopy (COSY) measurements, and confirmed by an X-ray diffraction study. The results of the latter are described before discussion of the NMR data for complexes **7**.

The structure of compound **7b** is shown in Fig. 1, and selected internuclear distances and angles are given in Table 3. The quality of the X-ray data allowed refinement of the hydrogen atoms bonded to the borons. It will be seen that the structure of the molecule may be described as an ion pair in which a [*nido*-7,8-C$_2$B$_9$H$_{10}$Me$_2$]$^-$ anion formally donates four electrons to a [W(CO)$_2$(η-C$_5$Me$_5$)]$^+$ fragment *via* two B–H$\rightharpoonup$W 3c-2e bonds. However, assignment of formal negative and positive charges to the carbaborane cage and to the tungsten–ligand fragment in this way should be treated with some caution. It is noteworthy that the η-C$_5$Me$_5$ ring tends towards co-ordination to the W atom in an η^3 rather than an η^5 bonding mode, since the W–C(24) [2.392(8)] and W–C(25) [2.415(8)] separations are somewhat longer than the W–C(21) [2.292(8)], W–C(22) [2.280(8)] and W–C(23) [2.280(7) Å] distances.

A significant feature of the structure of compound **7b** is that both B–H$\rightharpoonup$W bonds involve boron atoms [B(4) and B(5)] lying in the open pentagonal $\widehat{\mathrm{CCBBB}}$ face of the cage. This will be referred to further when the NMR data are discussed, and also when another *exo-nido*-tungstacarbaborane structure is described.

Formation of the compounds **7** by addition of HBF$_4$·Et$_2$O to

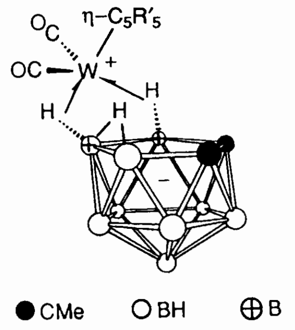

	R'
7a	H
7b	Me

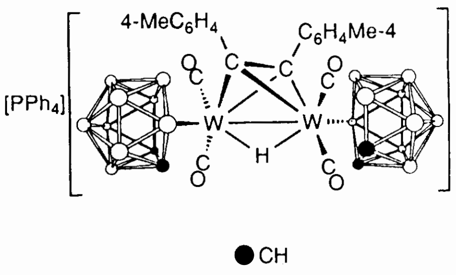

8

Table 2 Hydrogen-1 and carbon-13 NMR data[a] for the complexes

Compound	^{1}H (δ)[b]	^{13}C (δ)[c]
3b	−8.58 [q br, 1 H, BHW, J(BH) 70], 2.58 (s, 3 H, Me-4), 5.33 (s, 5 H, C_5H_5), 6.90, 7.40 [$(AB)_2$, 4 H, C_6H_4, J(AB) 8]	367.5 (μ-C), 218.7, 213.6, 209.6 (3 WCO), 163.0 [$C^1(C_6H_4)$], 137.0 [$C^4(C_6H_4)$], 128.5 [$C^3(C_6H_4)$], 120.9 [$C^2(C_6H_4)$], 92.7 (C_5H_5), 40.0, 39.1 [br, $CH(C_2B_9H_{11})$], 21.3 (Me-4)
7a	−10.75 [q br, 1 H, B(5)HW, J(BH) 70], −4.14 [vbr, 1 H, B(3)HB(4)], −3.00 [q br, 1 H, B(4)HW, J(BH) 101], 1.72 (s, 6 H, CMe), 6.02 (s, 5 H, C_5H_5)	235.4, 233.2 (CO), 95.7 (C_5H_5), 74.9, 66.9 (*C*Me), 22.4, 22.1 (C*Me*)
7b	−9.24 [q br, 1 H, B(5)HW, J(BH) 76], −3.76 [m, vbr, 2 H, B(4)HW and B(3)HB(4)], 1.57, 1.69 (s, 3 H, CMe), 2.16 (s, 15 H, C_5Me_5)	240.1 [CO, J(WC) 166], 239.1 [CO, J(WC) 171], 109.8 (C_5Me_5), 73.9, 65.5 (*C*Me), 22.4, 21.9 (C*Me*), 11.8 ($C_5\mathit{Me}_5$)
9[d]	−10.60 [q, br, 1 H, BHW, J(BH) 80], −6.42* (s, 1 H, WH), −2.79 (q, vbr, 1 H, BH_{endo}), 2.30 (m, 4 H, BCH_2), 2.32 (s, 6 H, Me-4), 5.25, 5.31* (s, 5 H, C_5H_5), 6.86, 7.02 [$(AB)_2$, 8 H, C_6H_4, J(AB) 8], 7.07* (m, C_6H_4)	218.4 [CO, J(WC) 171], 143.0 [$C^1(C_6H_4)$], 135.2 [$C^4(C_6H_4)$], 130.5 [$C^2(C_6H_4)$], 129.1 [$C^3(C_6H_4)$], 94.4*, 91.2 (C_5H_5), 83.8*, 61.1 [$CH(C_2B_9H_{11})$], 26.1 (vbr, BCH_2), 21.1 (Me-4)

[a] Chemical shifts (δ) in ppm, coupling constants in Hz. Measurements in CD_2Cl_2 at ambient temperatures. [b] Resonances due to terminal cage BH vertices occur as broad peaks in the range *ca.* 0–2.5. The following chemical shifts were assigned from ^{11}B–^{1}H COSY spectra (see Fig. 2): **7a**, 0.87 [vbr, 1 H, B(11)H], 0.97 [vbr, 1 H, B(3)H], 1.42 [vbr, 1 H, B(8)H], 1.60 [vbr, 1 H, B(6)H], 1.88 [vbr, 1 H, B(10)H], 1.88 [vbr, 1 H, B(7)H] and 2.24 [vbr, 1 H, B(9)H]; **7b** 0.99 [vbr, 1 H, B(11)H], 0.99 [vbr, 1 H, B(3)H], 1.54 [vbr, 1 H, B(8)H], 1.85 [vbr, 1 H, B(10)H], 1.93 [vbr, 1 H, B(6)H], 2.01 [vbr, 1 H, B(7)H] and 2.40 [vbr, 1 H, B(9)H]. [c] Hydrogen-1 decoupled, chemical shifts are positive to high frequency of $SiMe_4$ (0.0 ppm). [d] Peaks due to minor isomer (see text) indicated with an asterisk.

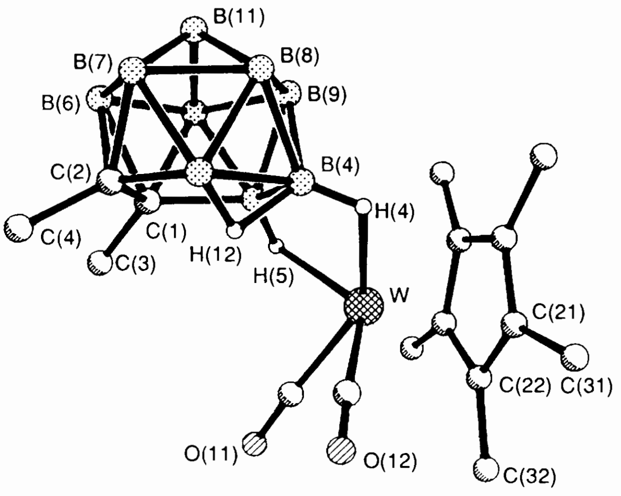

Fig. 1 Molecular structure of [*exo-nido*-9,10-{W(CO)$_2$(η-C_5Me_5)}-9,10-(μ-H)$_2$-7,8-$C_2B_9H_8$-7,8-Me_2] **7b**, showing the crystallographic labelling scheme

the salt **1c** in the presence of the compounds [W(≡CC_6H_4Me-4)(CO)$_2$(η-$C_5R'_5$)] (R' = H or Me) implies transfer of the η^5-7,8-$C_2B_9H_9Me_2$ ligand from molybdenum to tungsten, and the concomitant loss of two CC_6H_4Me-4 groups and a Mo(CO){P(OMe)$_3$} fragment. Although the pathway to complexes **7** is obscure at the present time, it seems very likely that a dimetal Mo–W species is an intermediate. Coupling of the two alkylidyne groups at adjacent metal centres to give the alkyne $C_2(C_6H_4Me\text{-}4)_2$ has ample precedent,[4] while transfer of the carbaborane cage from molybdenum to tungsten would be facilitated in a Mo–W intermediate by formation of an exo-polyhedral B–H⇀W bond.[3a,5] The molybdenum might be ejected as a Mo(CO){P(OMe)$_3$}{η-$C_2(C_6H_4Me\text{-}4)_2$} fragment which might scavenge CO from solution, forming species not isolated.

The NMR data for compounds **7a** and **7b** (Table 2) are extremely similar and reveal that, in solution, static structures are adopted of the type established by X-ray diffraction for **7b**. The NMR data for **7a** were of particularly high quality and are discussed below. Moreover, as mentioned above, the NMR data were sufficiently informative to establish the structures prior to the X-ray study.

The ^{13}C-{^{1}H} NMR spectrum of compound **7a** shows two resonances at δ 235.4 and 233.2 for the inequivalent CO ligands and the observation of pairs of *C*Me (δ 74.9 and 66.9) and C*Me* (δ 22.4 and 22.1) signals further confirms the asymmetry of the complex. The ^{1}H NMR spectrum shows two characteristic

Table 3 Selected internuclear distances (Å) and angles (°) for the complex [*exo-nido*-9,10-{$W(CO)_2(\eta-C_5Me_5)$}-9,10-(μ-H)$_2$-7,8-$C_2B_9H_8$-7,8-Me_2] **7b**

W–C(11)	1.934(9)	W–C(12)	1.953(11)	W–C(21)	2.292(8)	W–C(22)	2.280(8)
W–C(23)	2.280(7)	W–C(24)	2.392(8)	W–C(25)	2.415(8)	W–B(4)	2.50(1)
W–B(5)	2.38(1)	W–H(4)	2.16(8)	W–H(5)	1.95(7)	C(11)–O(11)	1.15(1)
C(12)–O(12)	1.13(1)	C(1)–C(2)	1.56(1)	C(1)–C(3)	1.49(1)	C(1)–B(5)	1.64(1)
C(1)–B(6)	1.73(1)	C(1)–B(10)	1.76(2)	C(2)–C(4)	1.51(2)	C(2)–B(3)	1.64(2)
C(2)–B(6)	1.73(2)	C(2)–B(7)	1.67(2)	B(3)–B(4)	1.84(2)	B(3)–B(7)	1.80(2)
B(3)–B(8)	1.81(2)	B(3)–H(12)	1.07(8)	B(4)–B(5)	1.71(2)	B(4)–B(8)	1.80(2)
B(4)–B(9)	1.81(2)	B(4)–H(12)	1.36(8)	B(5)–B(9)	1.74(1)	B(5)–B(10)	1.76(2)
B(6)–B(7)	1.74(2)	B(6)–B(10)	1.77(2)	B(6)–B(11)	1.76(2)	B(7)–B(8)	1.78(2)
B(7)–B(11)	1.74(2)	B(8)–B(9)	1.79(2)	B(8)–B(11)	1.77(2)	B(9)–B(10)	1.75(2)
B(9)–B(11)	1.74(1)	B(10)–B(11)	1.79(2)				

C(11)–W–C(12)	74.3(4)	C(11)–W–B(4)	121.4(4)	C(12)–W–B(4)	89.5(4)
C(11)–W–B(5)	94.6(4)	C(12)–W–B(5)	113.0(4)	B(4)–W–B(5)	41.0(4)
C(11)–W–H(4)	139(2)	C(12)–W–H(4)	83(2)	B(4)–W–H(4)	23(2)
B(5)–W–H(4)	63(2)	C(11)–W–H(5)	76(2)	C(12)–W–H(5)	127(2)
B(4)–W–H(5)	71(2)	B(5)–W–H(5)	30(2)	H(4)–W–H(5)	92(3)
W–C(11)–O(11)	175.1(8)	W–C(12)–O(12)	175.9(9)	C(2)–B(3)–H(12)	92(4)
B(4)–B(3)–H(12)	47(4)	B(7)–B(3)–H(12)	136(4)	B(8)–B(3)–H(12)	106(4)
H(3)–B(3)–H(12)	98(5)	W–B(4)–B(3)	132.4(8)	W–B(4)–B(5)	65.8(5)
W–B(4)–B(8)	165.8(8)	W–B(4)–B(9)	106.6(6)	W–B(4)–H(4)	59(5)
B(3)–B(4)–H(4)	125(5)	B(5)–B(4)–H(4)	121(5)	B(8)–B(4)–H(4)	123(5)
B(9)–B(4)–H(4)	121(4)	W–B(4)–H(12)	98(3)	B(3)–B(4)–H(12)	35(3)
B(5)–B(4)–H(12)	96(3)	B(8)–B(4)–H(12)	95(3)	B(9)–B(4)–H(12)	131(3)
H(4)–B(4)–H(12)	109(5)	W–B(5)–C(1)	131.4(6)	W–B(5)–B(4)	73.2(5)
W–B(5)–B(9)	114.4(6)	W–B(5)–B(10)	164.4(7)	W–B(5)–H(5)	54(3)
C(1)–B(5)–H(5)	112(4)	B(4)–B(5)–H(5)	127(4)	B(9)–B(5)–H(5)	132(4)
B(10)–B(5)–H(5)	117(4)	W–H(4)–B(4)	98(5)	W–H(5)–B(5)	96(4)
B(3)–H(12)–B(4)	98(6)				

quartet resonances for the B–H→W groups at δ −10.75 [B(5), *J*(BH) 70] and −3.00 [B(4), *J*(BH) 101 Hz] respectively, and a broad resonance for the *endo*-B(3)–H(12)–B(4) proton occurs at δ −4.14. Other resonances due to the cage BH protons occur as extremely broad peaks in the range δ *ca.* 0–2.5 and their chemical shifts were established from the ^{11}B–^{1}H and ^{11}B–^{11}B COSY NMR experiments described below. The correlation spectra are shown in Fig. 2 together with the unique connectivity map established from the experimental data. In the connectivity map bold lines show connectivities deduced from the presence of peaks in the COSY spectra and dotted lines show connections for which no coupling was observed. It is noteworthy that in the ^{11}B–^{11}B COSY spectrum no coupling was observed between B(3) and B(4). These two atoms are bridged by the *endo*-hydrogen atom H(12) and are therefore part of a 3c–2e B(3)–H–B(4) bond. With few exceptions, ^{11}B–^{11}B coupling is not observed in such situations,[6] which is consistent with calculations revealing that electron density along the B–B vector is small for B–H–B bonds.[7]

The addition of $HBF_4 \cdot Et_2O$ to a mixture of compounds **1d** and [$W(\equiv CMe)(CO)_2(\eta-C_5H_5)$] in CH_2Cl_2 at −78 °C was also investigated, and found to give the ditungsten compound [$W_2(\mu-CC_6H_4Me-4)(CO)_3(\eta^5-C_2B_9H_{11})(\eta-C_5H_5)$] **3b**, fully characterised by microanalysis and by spectroscopic data (Tables 1 and 2). Formation of **3b** results from loss of a CMe group from the precursor [$W(\equiv CMe)(CO)_2(\eta-C_5H_5)$], and the overall stoichiometry suggests that the ethylidyne ligand is released at some stage in the reaction profile as the ethylidene fragment C(H)Me. We have commented earlier on the similar loss of a $C(H)C_6H_4Me-4$ moiety in the synthesis of **3a** by treating a mixture of the salt **1b** and [$W(\equiv CC_6H_4Me-4)(CO)_2(\eta-C_5H_5)$] with $HBF_4 \cdot Et_2O$.

The ^{1}H NMR spectrum of compound **3b** shows a diagnostic resonance for the B–H→W group at δ −8.58 which appears as a quartet [*J*(BH) 70 Hz]. The presence of the B–H→W group was further confirmed from the ^{11}B-{^{1}H} NMR spectrum which revealed a characteristic signal corresponding in intensity to one boron nucleus at δ 15.9. The NMR data for the B–H→W group in **3a** are very similar: ^{1}H, δ −8.60 [*J*(BH) 75 Hz]; ^{11}B-{^{1}H}, δ 16.8.[3a]

Although compound **3b** is formed in high yield when mixtures of **1d** and [$W(\equiv CMe)(CO)_2(\eta-C_5H_5)$] are protonated with $HBF_4 \cdot Et_2O$ at −78 °C, in reactions carried out at room temperature a mixture of **3b** and an unidentified product was obtained, both formed in low yields (*ca.* 10%). The unidentified complex could not be isolated in a satisfactorily pure form, nevertheless crude NMR data suggested that it exists as an equilibrium mixture of two isomers, one species having an *exo-nido*-tungstacarbaborane structure and the other a *closo* structure. In particular, in the ^{1}H NMR spectrum a broad signal at δ −10.77 is diagnostic for a B–H→W linkage, a singlet at δ −6.48 is attributed to a terminal W–H unit, and a broad signal at δ −3.09 is ascribed to an *endo*-BH proton lying over the face of a *nido*-C_2B_9 cage. Furthermore, the ^{11}B-{^{1}H} NMR spectrum displayed high-field chemical shifts associated with the open face of a *nido* or *exo-nido* cage, notably at δ −35.6, −42.7 and −54.1. The significance of these ^{1}H and ^{11}B-{^{1}H} NMR data will be apparent following discussion of other work reported below.

The protonation of mixtures of compounds **1d** and [$W(\equiv CC_6H_4Me-4)(CO)_2(\eta-C_5H_5)$] with $HBF_4 \cdot Et_2O$ in CH_2Cl_2 was next investigated. The nature of the products isolated was found to be dependent on the temperature at which the reaction was carried out. At −78 °C the ditungsten salt [PPh_4][$W_2(\mu-H)\{\mu-C_2(C_6H_4Me-4)_2\}(CO)_4(\eta^5-C_2B_9H_{11})_2$] **8** was obtained, together with unreacted [$W(\equiv CC_6H_4Me-4)(CO)_2(\eta-C_5H_5)$]. The $[X]^+$ [X = $N(PPh_3)_2$ or NEt_4] analogues of **8** has been isolated and characterised previously from the reactions between [X][$W(\equiv CC_6H_4Me-4)(CO)_2(\eta^5-C_2B_9H_{11})$] and $HBF_4 \cdot Et_2O$.[8] It is likely that the μ-alkyne-ditungsten species $[W_2(\mu-H)\{\mu-C_2(C_6H_4Me-4)_2\}(CO)_4(\eta^5-C_2B_9H_{11})_2]^-$ forms *via* co-ordination of the anion $[W(\equiv CC_6H_4Me-4)(CO)_2(\eta^5-C_2B_9H_{11})]^-$ to an alkylidene complex [$W\{=C(H)C_6H_4Me-4\}(CO)_2(\eta^5-C_2B_9H_{11})$] initially produced by protonation. This step might be followed by C–C coupling and hydrogen migration from the resulting μ-vinyl group to give **8** or the $[X]^+$

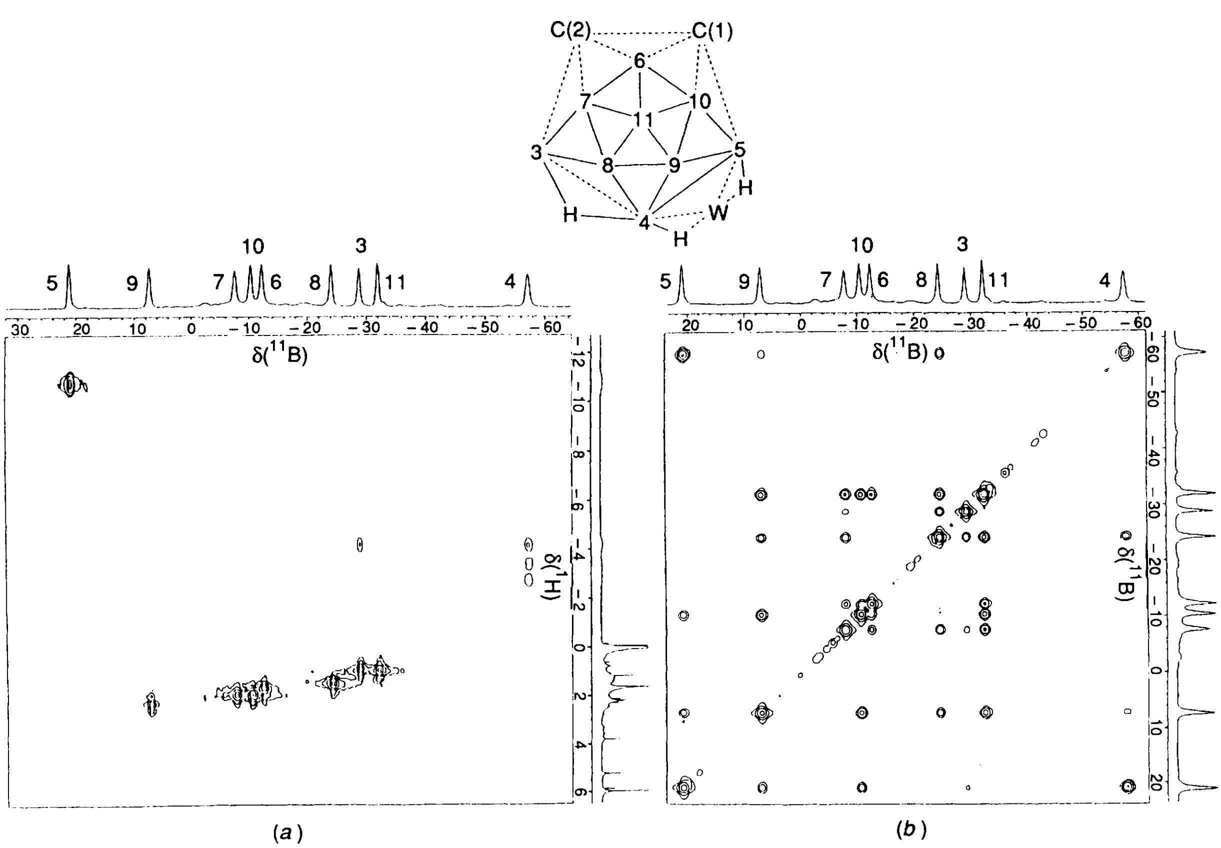

Fig. 2 The ^{11}B–^{1}H (*a*) and ^{11}B–^{11}B (*b*) COSY 90 NMR spectra of [*exo-nido*-9,10-{W(CO)$_2$(η-C$_5$H$_5$)}-9,10-(μ-H)$_2$-7,8-C$_2$B$_9$H$_8$-7,8-Me$_2$] **7a**. The numbering scheme used in the connectivity map is the same as that adopted in the crystal structure determination and bold lines show connections deduced from the COSY experiments. All *exo* cage hydrogens have been omitted with the exception of those on B(4) and B(5) which undergo B–H→W interactions

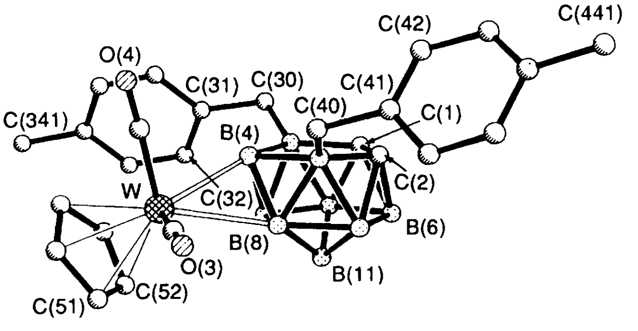

Fig. 3 Molecular structure of [*exo-nido*-9,11-(CH$_2$C$_6$H$_4$Me-4)$_2$-5,10-{W(CO)$_2$(η-C$_5$H$_5$)}-5,10-(μ-H)$_2$-7,8-C$_2$B$_9$H$_8$] **9a**, showing the crystallographic labelling scheme

analogue, as discussed elsewhere.[9] In the formation of **8** it is surprising that the presence of the reagent [W(≡CC$_6$H$_4$Me-4)(CO)$_2$(η-C$_5$H$_5$)] does not intervene in one of the reaction steps to afford a ditungsten analogue of one or other of the complexes **2** or **3**. This result suggests that the outcome of such protonations is highly sensitive to the relative rates of several steps along the reaction pathway. Suspecting that this may lead to temperature dependence, the same reaction was repeated, but at *ca.* +20 °C. A remarkably different result was thereby obtained.

Treatment of a mixture of compounds **1d** and [W(≡CC$_6$H$_4$Me-4)(CO)$_2$(η-C$_5$H$_5$)] with HBF$_4$·Et$_2$O at ambient temperatures gave a red crystalline product **9**. Examination of the NMR spectra revealed that it was formed as an equilibrium mixture of two isomers in solution but with one species predominating (*ca.* 10:1). It was possible to carry out an X-ray diffraction study on the major isomer which led to its identification as [*exo-nido*-9,11-(CH$_2$C$_6$H$_4$Me-4)$_2$-5,10-{W(CO)$_2$(η-C$_5$H$_5$)}-5,10-(μ-H)$_2$-7,8-C$_2$B$_9$H$_8$] **9a**. Only small and relatively poor quality crystals could be obtained despite persistent efforts and problems arose during the refinement. Nevertheless, the gross geometry of **9a** was clearly revealed, and is fully supported by the spectroscopic data discussed later.

The molecule is shown in Fig. 3 and selected structural parameters are given in Table 4. Two important structural features are immediately apparent. The cage has a *nido*-C$_2$B$_9$ framework with CH$_2$C$_6$H$_4$Me-4 substituents attached to the boron atoms B(3) and B(5) in the open pentagonal $\overline{\mathrm{CCBBB}}$ face. Moreover, the remaining boron [B(4)] in this face, and B(8) in the B$_5$ pentagonal layer, are attached to an exo-polyhedral W(CO)$_2$(η-C$_5$H$_5$) fragment. The hydrogen atoms bonded to the borons in **9a** were not located in the X-ray electron-density maps nor were they included in the calculations. However, from the NMR data, discussed below, the tungsten atom is co-ordinated to the cage *via* two 3c–2e B–H→W bonds. This conformation is in contrast with the structure of **7b**, where both B–H→W linkages involve borons in the pentagonal face of the *nido*-C$_2$B$_9$ cage. Clearly **9a** could not have an *exo-nido* structure similar to **7b** because two boron atoms [B(3) and B(5)] in the *nido* face of the cage carry CH$_2$C$_6$H$_4$Me-4 substituents, thus preventing formation of two B–H→W linkages from this ring. Complex **9a** must also contain an *endo*-hydrogen in the open $\overline{\mathrm{CCBBB}}$ face, and we favour the idea that it is attached to B(4), making this boron part of a BH$_2$ group. A recent structural study on the parent anion [*nido*-7,8-C$_2$B$_9$H$_{12}$]$^-$ revealed the presence of a BH$_2$ unit in the open $\overline{\mathrm{CCB}B\mathrm{B}}$ face of the cage, and not as previously thought a hydrogen forming a B–H–B bridge system.[10]

Examination of the NMR spectra of compound **9** revealed that this product displays dynamic behaviour in solution involving a facile fluxional process for the major isomer **9a**,

Table 4 Selected internuclear distances (Å) and angles (°) for the complex [*exo-nido*-9,11-($CH_2C_6H_4Me$-4)$_2$-5,10-{W(CO)$_2$(η-C_5H_5)}-5,10-(μ-H)$_2$-7,8-$C_2B_9H_8$] **9a**

W–C(3)	1.99(3)	W–C(4)	1.968(9)[a]	W–B(4)	2.53(3)	W–B(8)	2.55(2)
C(3)–O(3)	1.14(4)	C(4)–O(4)	1.15(1)[a]	C(1)–C(2)	1.58(3)	W–C(cp)	2.31[b]
C(1)–B(5)	1.58(3)	C(1)–B(6)	1.73(3)	C(1)–B(10)	1.72(2)	C(2)–B(3)	1.57(4)
C(2)–B(6)	1.71(3)	C(2)–B(7)	1.71(4)	B(3)–B(4)	1.91(3)	B(3)–B(7)	1.76(3)
B(3)–B(7)	1.76(3)	B(3)–B(8)	1.80(3)	B(3)–C(40)	1.62(3)	B(4)–B(5)	1.86(5)
B(4)–B(8)	1.72(3)	B(4)–B(9)	1.80(3)	B(5)–B(9)	1.81(4)	B(5)–B(10)	1.75(3)
B(5)–C(30)	1.57(4)	B(6)–B(7)	1.78(4)	B(6)–B(10)	1.83(3)	B(6)–B(11)	1.81(4)
B(7)–B(8)	1.72(3)	B(7)–B(11)	1.86(3)	B(8)–B(9)	1.80(3)	B(8)–B(9)	1.80(3)
B(8)–B(11)	1.78(3)	B(9)–B(10)	1.70(4)	B(9)–B(11)	1.62(3)	B(10)–B(11)	1.73(4)
C(30)–C(31)	1.51(3)	C(40)–C(41)	1.54(3)				

C(3)–W–C(4)	72.6(8)	C(3)–W–B(4)	117.5(9)	C(4)–W–B(4)	90.8(6)
C(3)–W–B(8)	94.1(9)	C(4)–W–B(8)	115.2(5)	B(4)–W–B(8)	39.6(7)
W–C(3)–O(3)	179(2)	W–C(4)–O(4)	177(1)	C(2)–B(3)–C(40)	125(2)
B(4)–B(3)–C(40)	123(2)	B(7)–B(3)–C(40)	122(2)	B(8)–B(3)–C(40)	125(2)
W–B(4)–B(3)	101(1)	W–B(4)–B(5)	153(1)	C(1)–B(5)–C(30)	124(5)
B(4)–B(5)–C(30)	122(2)	B(9)–B(5)–C(30)	128(2)	B(10)–B(5)–C(30)	123(2)
B(3)–C(40)–C(41)	113(2)	B(5)–C(30)–C(31)	115(2)		

[a] Constrained length (see Experimental section). [b] Average distance between W and C atoms of C_5H_5 ring.

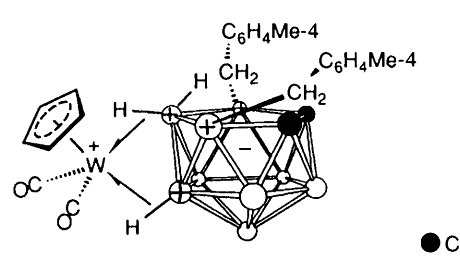

9a

●CH ○BH ⊕B

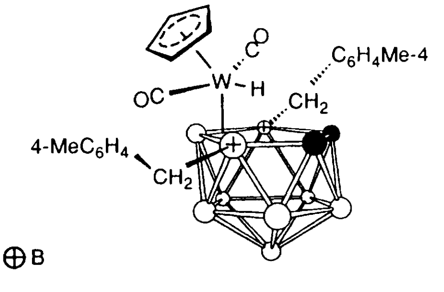

9b

coupled with a slower equilibration with the minor isomer **9b** discussed below. Unfortunately, limiting low-temperature ^1H and ^{13}C-{^1H} NMR spectra of the isomeric mixture could not be obtained at −80 °C. Nevertheless, structural features revealed by the X-ray diffraction study of **9a** were identifiable in the ambient-temperature NMR spectra (Table 2). Fluxionality of **9a** in solution leads to the time-averaged appearance of a mirror plane through B(4), B(6) and B(11) (Fig. 3). Thus in the ^{13}C-{^1H} NMR spectrum one set of signals is observed for the groups BCH_2 (δ 26.1), C_6H_4 (δ 129.1–143.0) and Me-4 (δ 21.1). The cage CH vertices also give rise to a single resonance (δ 61.1), as do the C_5H_5 ring carbons (δ 91.2), and the CO groups (δ 218.4). It is noteworthy that in the IR spectrum (Table 1) several CO bands occur. In the ^{11}B-{^1H} NMR spectrum the BCH_2 groups are revealed by a peak at δ 2.75, but the boron atoms involved in the B–H⇀W bonds are not identifiable as they do not appear with uniquely deshielded shifts, as is generally observed.[3,5] This is perhaps not surprising in view of the highly unusual nature of this cage structure, which gives rise to a greater range of resonances than is observed for *closo* icosahedra. In particular, ^{11}B signals are observed at significantly higher field *e.g.* δ −35.9, −42.4 and −53.6. The ^1H NMR spectrum reveals the existence of a B–H⇀W interaction, with a typical broad quartet at δ −10.60 [*J*(BH) 80 Hz]. However, since the hydrogen atoms exopolyhedrally bound to B(4) and B(8) apparently must always be chemically non-equivalent, two such signals would be expected. Two obvious explanations arise immediately. First, the two signals may be fortuitously coincident, and the peak integration of such a broad and weak resonance is unreliable. This is considered improbable. Secondly, the missing signal may, by virtue of the *exo-nido* structure, be uncommonly deshielded, and may therefore be masked by the very broad terminal B–H proton resonances. However, the favoured explanation involves consideration of the possible mechanisms of dynamic behaviour discussed below. First it is appropriate to relate the crystal structures of compounds **7b** and **9a** to those of other *exo-nido*-metallacarbaboranes.

The structure of compound **7b**, with two B–H⇀W bonds involving boron atoms in the open $\overline{\text{CCBBB}}$ face of the cage, is similar to that of the compound [*exo-nido*-9,10-($AlMe_2$)-9,10-(μ-H)$_2$-7,8-$C_2B_9H_{10}$] **10**, prepared by treating $C_2B_9H_{13}$ with $AlMe_3$.[11] In contrast, the *exo-nido* polyhedral structure of **9a** is related to those of several iridium– and rhodium–carbaborane complexes studied by Hawthorne and his co-workers,[12] *e.g.* compounds **11** and **12a**. In these species [Rh(PR_3)$_2$]$^+$ and [IrH_2(PR_3)$_2$]$^+$ (R = alkyl or aryl) fragments are bonded to various [*nido*-$C_2B_9H_{10}R'R''$]$^-$ (R′ or R″ = H, Me, or Ph; R′R″ = μ-1′,2′-$CH_2C_6H_4CH_2$) anions. By altering the substituents on the cage-carbon atoms and on the phosphine ligand, it was possible to demonstrate a general pattern of fluxional behaviour, as well as tautomerism between *exo-nido* and *closo* structures. Thus solution NMR studies revealed that **12a** exists in equilibrium with **12b**. Interconversion between tautomers on the NMR time-scale is slow, but the *exo-nido* species **12a** displays a facile fluxional process in which the [Rh(PPh_3)$_2$]$^+$ group interacts with pairs of cage BH vertices. Moreover, in certain complexes it was shown that the *endo*-BH proton scrambles over the BH vertices. There is a delicate energy balance between the various structures. Thus the equilibrium mixture of **12a** and **12b** yields crystals of **12a**, whereas other systems afford crystals of *closo* structures akin to **12b**.

These various observations allow an understanding of the dynamic behaviour of compound **9**. Thus the fluxional mechanism for **9a** shown in Scheme 1, in which the [W(CO)$_2$(η-C_5H_5)]$^+$ fragment rotates by 'stepping' around a triangular face of the cage, would lead to the aforementioned time-averaged mirror plane through the molecule, with the consequential apparent equivalence of certain NMR resonances. Secondly, the observation of only one B–H→W signal in the ^{1}H NMR spectrum may be explained by rapid scrambling of the hydrogen atoms associated with this triangular face, including the *endo*-BH hydride as observed with the *exo-nido* $[Rh(PR_3)_2]^+$ species. Thirdly, a number of small peaks observed in the NMR spectrum of **9** may be assigned to the presence of **9b**, the *closo* tautomer of **9a**. As mentioned earlier, relative peak intensities indicate a *ca.* 10:1 ratio in favour of **9a**. Evidence for **9b** comes principally from the ^{1}H NMR spectrum (Table 2). Thus a small but sharp resonance at δ −6.42 is ascribed to a terminal W–H group. Signals due to the C_5H_5 and C_6H_4 aromatic protons were also observed, but the remaining peaks were too weak to be detected, or were coincident with signals for **9a**. The same causes are probably responsible for the observation of only two resonances for the minor isomer **9b** in the $^{13}C\text{-}\{^1H\}$ NMR spectrum. These are the signals for the C_5H_5 (δ 94.4) and cage-CH nuclei (δ 83.8). The unusually high frequency for the latter peak is tentatively ascribed to an η^3-bonding mode for the cage, which does not involve significant carbon–tungsten interactions. Thus although the structure proposed for the minor product **9b** is based on somewhat tenuous evidence, the available data fit well with the results of Hawthorne and co-workers[12b,c] for the rhodium systems.

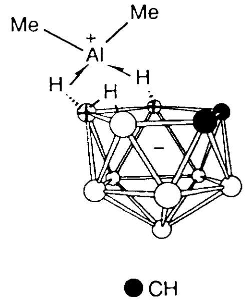

10

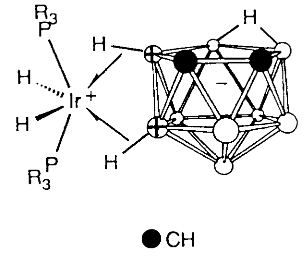

11 R = C_6H_4Me-4 or Ph

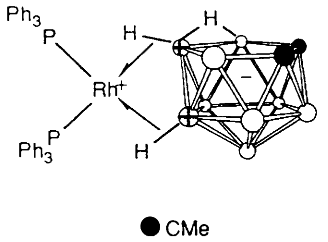

12a

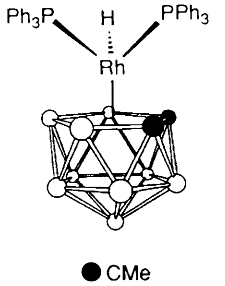

12b

Although compound **9a** displays fluxional behaviour, there is little evidence that the complexes **7** do so, a fact that is somewhat surprising. However, examination of the ^{1}H and COSY NMR spectra of **7a** and **7b** do reveal the presence of minor species. In the ^{1}H NMR spectrum of **7a** a very weak but sharp signal at δ −7.37 is probably due to a W–H group present in a *closo* structure akin to **9b**. This feature is absent from the ^{1}H NMR spectrum of **7b**, but the $^{11}B\text{-}^1H$ COSY NMR spectrum shows two minor species, each of which has a B–H→W resonance at δ −9 to −10 and another similar signal at δ −2 to −3 on the hydrogen axis. In addition, each of these minor species shows a resonance due to a BH_2 group at *ca.* δ −2.5 and δ −4.0 on the same axis. Clearly both these minor species are *exo-nido* compounds, but whether isomers in slow exchange with **7b** or distinct complexes perhaps similar to **9a** cannot be ascertained.

Compound **9a** is evidently formed by a very complicated pathway, which must involve several intermediates, the structures of which are unknown at the present time. As in the formation of the complexes **7**, the synthesis of **9a** involves transfer of an η^5-C_2B_9 cage from one metal centre to another, a process very likely to occur *via* the intermediacy of a dimetal species. However, in contrast with the steps leading to **7**, the alkylidyne groups are not ejected but appear as $CH_2C_6H_4Me$-4 substituents on cage boron atoms. There are now numerous known examples of reactions of the salts **1** with acids which lead to conversion of alkylidyne ligands into $CH_2C_6H_4Me$-4 groups attached to a boron vertex.[1–3] Molecule **9a** is, however, without precedent since it contains two such fragments, and unlike all preceding examples these are found on boron atoms adjacent to the cage carbons.

The various reactions reported herein amply demonstrate

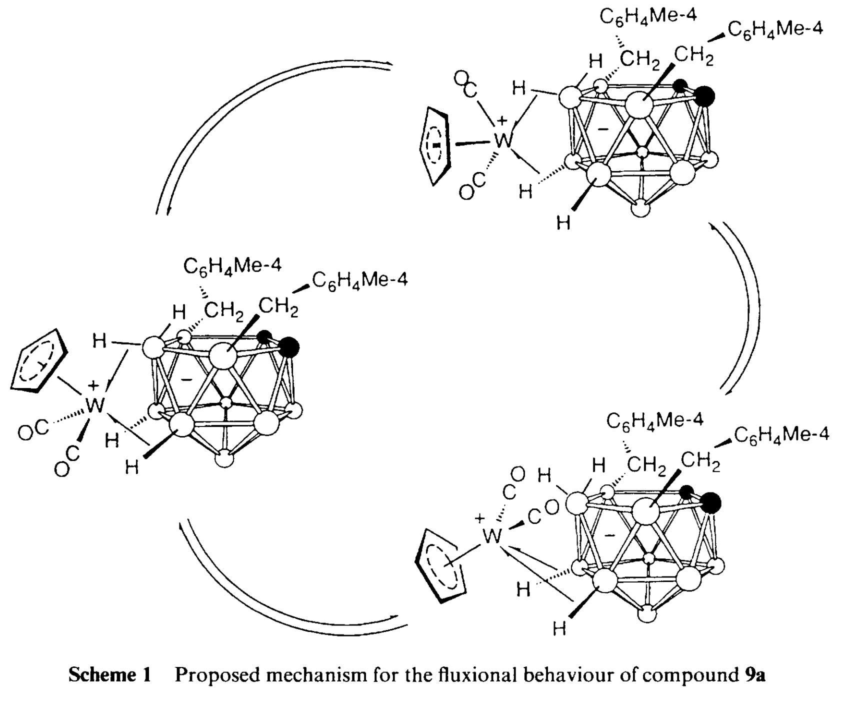

Scheme 1 Proposed mechanism for the fluxional behaviour of compound **9a**

Table 5 Data for crystal-structure analyses[a]

	7b	**9a**
Crystal dimensions/mm	0.65 × 0.25 × 0.18	0.10 × 0.20 × 0.20
Molecular formula	$C_{16}H_{31}B_9O_2W$	$C_{25}H_{33}B_9O_2W$
M	536.6	646.7
Crystal colour, shape	Purple needles	Red prisms
Crystal system	Monoclinic	Triclinic
Space group	$P2_1/n$	$P\bar{1}$
a/Å	8.991(3)	10.101(7)
b/Å	12.948(6)	12.22(1)
c/Å	19.679(7)	13.320(9)
α/°	90.00	109.32(6)
β/°	92.04(3)	89.99(6)
γ/°	90.00	113.24(6)
U/Å^3	2289(1)	1410(2)
Z	4	2
D_c/g cm^{-3}	1.56	1.52
μ(Mo-Kα)/cm^{-1}	51.6	42.0
F(000)	1048	636
T/K	293	293
Data collection limits/°	$5 \leqslant 2\theta \leqslant 50$	$5 \leqslant 2\theta \leqslant 55$
No. of unique data	4734	6111
No. of observed data used	2957	4009
Criterion for observed, *n* in $F_o \geqslant n\sigma(F_o)$	5	6
R (R')[b]	0.036 (0.037)	0.104 (0.099)
Final electron-density difference features (maximum, minimum), e Å^{-3}	1.20, −0.54	1.66, −1.70[c]

[a] Data collected on a Siemens R3m/V four-circle diffractometer operating in the Wyckoff ω-scan mode; graphite-monochromated Mo-Kα X-radiation, $\bar{\lambda}$ = 0.710 69 Å. Refinement was by full-matrix least-squares with a weighting scheme of the form $w^{-1} = [\sigma^2(F_o) + g|F_o|^2]$ with $g = 0.0005$ for **7b** and 0.006 for **9a**; $\sigma^2(F_o)$ is the variance in F_o due to counting statistics; *g* was chosen so as to minimize variation in $\Sigma w(|F_o| - |F_c|)^2$ with $|F_o|$. [b] $R = \Sigma||F_o| - |F_c||/\Sigma|F_o|$, $R' = \Sigma w^{\frac{1}{2}}||F_o| - |F_c||/\Sigma w^{\frac{1}{2}}|F_o|$. [c] Large residuals were also observed in the vicinity of the W atom (see Experimental section).

Table 6 Atomic positional parameters (fractional coordinates × 10^4) for compound **7b**, with estimated standard deviations (e.s.d.s) in parentheses

Atom	*x*	*y*	*z*
W	2174(1)	2102(1)	4405(1)
C(11)	137(10)	1700(8)	4198(4)
O(11)	−1059(7)	1477(8)	4026(4)
C(12)	2073(13)	630(8)	4612(5)
O(12)	2029(12)	−236(6)	4693(5)
C(21)	4074(9)	1732(7)	3698(4)
C(22)	2717(9)	1794(6)	3300(4)
C(23)	2214(9)	2838(6)	3353(4)
C(24)	3305(8)	3420(6)	3746(4)
C(25)	4446(8)	2738(7)	3937(4)
C(31)	5098(11)	804(8)	3726(6)
C(32)	2014(10)	982(7)	2866(4)
C(33)	878(10)	3306(8)	2973(5)
C(34)	3261(10)	4563(7)	3844(4)
C(35)	5883(9)	3044(8)	4302(5)
C(1)	362(10)	3024(7)	5935(4)
C(2)	946(12)	2375(7)	6554(4)
C(3)	−1236(11)	2920(8)	5724(6)
C(4)	−166(14)	1730(9)	6921(5)
B(3)	2589(17)	1879(11)	6422(6)
B(4)	3084(15)	2442(10)	5599(5)
B(5)	1574(11)	3169(8)	5343(5)
B(6)	829(13)	3691(10)	6676(5)
B(7)	2338(14)	2961(10)	6983(5)
B(8)	3776(12)	3007(10)	6382(5)
B(9)	3081(11)	3827(9)	5711(5)
B(10)	1273(12)	4222(9)	5882(5)
B(11)	2664(14)	4101(10)	6549(5)

how the nature of the products obtained on treatment of the salts **1** with $HBF_4 \cdot Et_2O$ are subtly influenced by the cage-carbon substituents, the character of the substrate molecules present, and reaction temperatures. Because of the complexity and variety of the products obtained, it is apparent that this is a fruitful area of study in uncovering new types of metallacarbaboranes.

Experimental

The instrumentation used for the spectroscopic measurements and the experimental techniques employed have been described in earlier papers.[2,3b] The tetrafluoroboric acid was an 85% solution of $HBF_4 \cdot Et_2O$ in Et_2O, as supplied by Aldrich Chemicals. The reagents **1b**–**1d** were made by procedures previously described for these and related species.[2b,13] Light petroleum refers to that fraction of b.p. 40–60 °C unless otherwise specified. Chromatography columns were packed with alumina (Aldrich, Brockmann Activity III) or silica (Fluka, Kieselgel 70–230 mesh). Analytical and other data for the new compounds are given in Table 1. The ^{11}B NMR measurements were made in CD_2Cl_2 at 160 MHz on a JEOL GX 500 MHz spectrometer and the chemical shifts (δ) are positive to high frequency of $BF_3 \cdot Et_2O$ (external, 0.0 ppm). The data were obtained from a combination of one- and two-dimensional techniques. For the boron atom numbering scheme see Fig. 2.

Reactions of the Salt $[NEt_4][Mo(\equiv CC_6H_4Me\text{-}4)(CO)\{P(OMe)_3\}(\eta^5\text{-}C_2B_9H_9Me_2)]$ **1c**.—(*i*) A mixture of $[W(\equiv CC_6H_4Me\text{-}4)(CO)_2(\eta\text{-}C_5H_5)]$ (0.27 g, 0.67 mmol) and the salt **1c** (0.43 g, 0.67 mmol) in CH_2Cl_2 (10 cm^3) was treated at −78 °C with $HBF_4 \cdot Et_2O$ (120 μl, 0.70 mmol) and stirred. The mixture was warmed slowly to room temperature, during which time the colour changed from red to dark brown. Solvent was removed *in vacuo*, the residue was dissolved in CH_2Cl_2–light petroleum (2 cm^3, 3:2), and chromatographed at −40 °C on a silica column (*ca.* 8 cm long and 2 cm diameter). Rapid elution with the same solvent mixture removed a blue eluate, part of which was observed to decompose on the column. Removal of solvent *in vacuo* gave oily blue *microcrystals* of [*exo-nido*-9,10-$\{W(CO)_2(\eta\text{-}C_5H_5)\}$-9,10-$(\mu\text{-}H)_2$-7,8-$C_2B_9H_8$-7,8-$Me_2$] **7a** (0.04 g). ^{11}B NMR: δ 21.0 [B(5)HW, *J*(HB) 70], 7.2 [B(9), *J*(HB) 147], −7.7 [B(7), *J*(HB) 159], −10.5 [B(10), *J*(HB) 162], −12.3 [B(6), *J*(HB) 174], −24.3 [B(8), *J*(HB) 146], −29.0 [*B*(3)HB(4), *J*(HB) 140 and 40], −32.1 [B(11), *J*(HB) 147] and −57.3 [br, B(3)H*B*(4)HW, *J*(HB) 101 Hz]. Crystals suitable for microanalysis were grown from a toluene solution layered with light petroleum (b.p. 30–40 °C).

(*ii*) Using a similar procedure, a mixture of $[W(\equiv CC_6H_4Me\text{-}4)(CO)_2(\eta\text{-}C_5Me_5)]$ (0.19 g, 0.40 mmol) and salt the **1c** (0.26 g, 0.40 mmol) in CH_2Cl_2 (10 cm^3) at −78 °C treated with $HBF_4 \cdot Et_2O$ (80 μl, 0.40 mmol) gave oily purple *microcrystals* of [*exo-nido*-9,10-$\{W(CO)_2(\eta\text{-}C_5Me_5)\}$-9,10-$(\mu\text{-}H)_2$-7,8-$C_2B_9H_8$-7,8-$Me_2$] **7b** (0.03 g). ^{11}B NMR: δ 11.3 [B(5)HW, *J*(HB) 76], 5.7 [B(9), *J*(HB) 143], −7.9 [B(7), *J*(HB) 159], −11.2 [B(10), *J*(HB) 140], −12.3 [B(6), *J*(HB) 171], −26.5 [B(8), *J*(HB) 137], −27.2 [*B*(3)HB(4)], −32.2 [B(11), *J*(HB) 143] and −50.1 [br, B(3)H*B*(4)HW, *J*(HB) 86 Hz]. Crystals for microanalysis and X-ray crystallography were grown from a toluene solution layered with light petroleum.

Reactions of the Salt $[PPh_4][W(\equiv CC_6H_4Me\text{-}4)(CO)_2(\eta^5\text{-}C_2B_9H_{11})]$ **1d**.—(*i*) A mixture of the salt **1d** (0.20 g, 0.25 mmol) and $[W(\equiv CMe)(CO)_2(\eta\text{-}C_5H_5)]$ (0.082 g, 0.25 mmol) in CH_2Cl_2 (20 cm^3) at −78 °C was treated with $HBF_4 \cdot Et_2O$ (50 μl, 0.29 mmol). The mixture darkened rapidly, and after 5 min an IR spectrum showed the reaction to be complete. Solvent was removed *in vacuo* and a mixture of CH_2Cl_2–hexane (3 cm^3, 2:3)

Table 7 Atomic positional parameters (fractional coordinates × 10^4) for compound **9a**, with e.s.d.s in parentheses

Atom	*x*	*y*	*z*
W	1564(1)	3581(1)	1220(1)
C(3)	870(25)	3682(22)	−128(19)
O(3)	490(18)	3759(17)	−894(13)
C(4)	−235(11)	2030(10)	529(14)
O(4)	−1316(11)	1157(10)	111(14)
C(1)	5279(23)	1602(19)	620(15)
C(2)	4670(21)	1608(18)	−466(14)
B(3)	3271(24)	1875(20)	−407(14)
B(4)	3003(25)	2256(20)	1068(15)
B(5)	4430(31)	1896(25)	1595(18)
B(6)	6305(26)	2830(23)	190(17)
B(7)	4943(27)	3106(23)	−394(16)
B(8)	3901(24)	3456(19)	582(12)
B(9)	4713(26)	3518(23)	1811(18)
B(10)	6123(26)	3091(19)	1603(18)
B(11)	5805(25)	4062(21)	1027(16)
C(30)	4159(26)	1219(20)	2442(16)
C(31)	3467(21)	1746(19)	3377(15)
C(32)	4303(27)	2887(22)	4246(16)
C(33)	3678(28)	3430(25)	5064(16)
C(34)	2158(31)	2846(26)	5064(18)
C(35)	1349(33)	1725(28)	4198(21)
C(36)	1915(30)	1192(26)	3378(18)
C(341)	1479(44)	3464(44)	5999(25)
C(40)	1933(25)	1239(22)	−1386(15)
C(41)	2287(25)	547(21)	−2478(16)
C(42)	2262(27)	−654(20)	−2703(18)
C(43)	2516(26)	−1275(23)	−3746(19)
C(44)	2820(31)	−761(32)	−4502(18)
C(45)	2865(35)	466(29)	−4241(18)
C(46)	2673(28)	1134(24)	−3262(17)
C(441)	3050(47)	−1484(38)	−5590(22)
C(51)	1832(25)	5609(18)	2123(15)
C(52)	2846(27)	5455(24)	2725(16)
C(53)	2182(25)	4562(19)	3153(14)
C(54)	607(29)	4050(23)	2768(16)
C(55)	499(24)	4816(19)	2183(16)

was added to the residue for transfer to the top of an alumina column (15 cm long and 2 cm diameter) using a syringe. Elution with the same solvent mixture afforded a green fraction. Removal of solvent *in vacuo* afforded dark green *microcrystals* of $[W_2(\mu\text{-}CC_6H_4Me\text{-}4)(CO)_3(\eta^5\text{-}C_2B_9H_{11})(\eta\text{-}C_5H_5)]$ **3b** (0.17 g), crystallised from CH_2Cl_2–hexane (10 cm^3, 1:10). $^{11}B\text{-}\{^1H\}$ NMR: δ 15.9 (1 B, BHW), −7.3, −9.2, −12.4, −13.4, −16.9, −18.3, −21.3 and −26.0 (1 B × 8).

(*ii*) A mixture of salt **1d** (0.12 g, 0.15 mmol) and $[W(\equiv CC_6H_4Me\text{-}4)(CO)_2(\eta\text{-}C_5H_5)]$ (0.080 g, 0.15 mmol) in CH_2Cl_2 (15 cm^3) at room temperature was treated with $HBF_4{\cdot}Et_2O$ (30 μl, 0.17 mmol). As before, rapid darkening of this mixture was observed and an IR spectrum showed the reaction to be complete within 5 min. Chromatography, as in the synthesis of **3b**, afforded a red fraction as the only isolable product. Solvent was removed *in vacuo* and the residue recrystallised from toluene–pentane (5 cm^3, 1:20) at −78 °C to afford deep red *microcrystals* of [*exo-nido*-9,11-$(CH_2C_6H_4\text{-}Me\text{-}4)_2$-5,10-$\{W(CO)_2(\eta\text{-}C_5H_5)\}$-5,10-$(\mu\text{-}H)_2$-7,8-$C_2B_9H_8$] **9a** (0.051 g). $^{11}B\text{-}\{^1H\}$ NMR (peaks with asterisks assigned to minor isomer **9b**): δ 25.3* (2 B, BCH_2), 2.8 (2 B, BCH_2), −1.6, −11.2* (1 B), −18.6, −20.7, −23.7, −25.4*, −28.9*, −29.8* (1 B × 3), −35.9, −37.8* (1 B), −42.4 and −53.6 (1 B × 2). Some peaks of the minor isomer are apparently hidden under the major signals.

Crystal Structure Determinations and Refinements.—The crystal data and experimental parameters for compounds **7b** and **9a** are given in Table 5. Crystals of **7b** were grown from toluene layered with light petroleum, and those of **9a** by diffusion of pentane into a toluene solution over several days. All data were corrected for Lorentz, polarisation and X-ray absorption effects, the latter by an empirical method based upon azimuthal scan data.[14] The structures were solved by conventional heavy-atom methods, and difference methods used to locate and refine anisotropically all non-hydrogen atoms.

For compound **7b** all methyl hydrogen atoms were included in calculated positions (C–H 0.96 Å) with chemically related hydrogen atoms having common refined isotropic thermal parameters. The positions of the BH hydrogen atoms were refined with fixed isotropic thermal parameters.

For compound **9a** hydrogen atoms were included in calculated positions (aromatic, methyl and methylene C–H 0.96; carbaborane C–H and B–H 1.1 Å), with fixed isotropic thermal parameters (U_{iso} 0.08 $Å^2$). However, for reasons that are still unclear, the refinement was not entirely satisfactory. In particular, the final electron-density difference synthesis showed large residual peaks (*ca.* 7.15 e $Å^{-3}$) close to the tungsten atom (*ca.* 0.9 Å), implying that absorption errors had been inadequately corrected. This necessitated constraint of the distances W–C(4) [1.968(2)], W···O(4) [3.12(1)] and C(4)–O(4) [1.153(2)]. Although peak profiles of the crystals, including the one eventually selected, were split, the reasons for the absorption correction failure remain unresolved. In the light of these problems, calculation of the hydrogen-atom positions for B(4) (*endo* and *exo*) and B(8) (*exo*) was not attempted. Furthermore it is evident that detailed discussion of the geometric parameters is not justified. However, the gross geometry is revealed and is fully supported by the spectroscopic data.

All computations were performed on a DEC μ-Vax II computer using the SHELXTL system of programs.[14] Scattering factors are included in the program and the atom coordinates are given in Tables 6 and 7.

Additional material available from the Cambridge Crystallographic Data Centre comprises H-atom coordinates, thermal parameters and remaining bond lengths and angles.

Acknowledgements

We thank the SERC for research studentships (to S. A. B. and M. D. M.) and Dr. M. Murray for assistance with the two-dimensional NMR studies.

References

1 Part 5, J. C. Jeffery, S. Li, D. W. I. Sams and F. G. A. Stone, *J. Chem. Soc., Dalton Trans.*, 1992, 877.

2 (*a*) S. A. Brew, D. D. Devore, P. D. Jenkins, M. U. Pilotti and F. G. A. Stone, *J. Chem. Soc., Dalton Trans.*, 1992, 393; (*b*) S. A. Brew, P. D. Jenkins, J. C. Jeffery and F. G. A. Stone, *J. Chem. Soc., Dalton Trans.*, 1992, 401.

3 (*a*) S. A. Brew, N. Carr, M. D. Mortimer and F. G. A. Stone, *J. Chem. Soc., Dalton Trans.*, 1991, 811; (*b*) S. A. Brew and F. G. A. Stone, *J. Chem. Soc., Dalton Trans.*, 1992, 867.

4 F. G. A. Stone and M. L. Williams, *J. Chem. Soc., Dalton Trans.*, 1988, 2467; S. J. Etches, I. J. Hart and F. G. A. Stone, *J. Chem. Soc., Dalton Trans.*, 1989, 2281 and refs. therein.

5 S. J. Dossett, I. J. Hart and F. G. A. Stone, *J. Chem. Soc., Dalton Trans.*, 1990, 3481.

6 T. L. Venable, W. C. Hutton and R. N. Grimes, *J. Am. Chem. Soc.*, 1984, **106**, 29.

7 E. Switkes, R. M. Stevens and W. N. Lipscomb, *J. Chem. Phys.*, 1969, **51**, 2085; E. Switkes, I. R. Epstein, J. A. Tossell, R. M. Stevens and W. N. Lipscomb, *J. Am. Chem. Soc.*, 1970, **92**, 3837; E. A. Laws, R. M. Stevens and W. N. Lipscomb, *J. Am. Chem. Soc.*, 1972, **94**, 4467.

8 A. P. James and F. G. A. Stone, *J. Organomet. Chem.*, 1986, **310**, 47; S. A. Brew, N. Carr, J. C. Jeffery, M. U. Pilotti and F. G. A. Stone, *J. Am. Chem. Soc.*, 1992, **114**, 2203.

9 J. A. K. Howard, J. C. Jeffery, J. C. V. Laurie, I. Moore, F. G. A. Stone and A. Stringer, *Inorg. Chim. Acta*, 1985, **100**, 23.

10 J. Buchanan, E. J. M. Hamilton, D. Reed and A. J. Welch, *J. Chem. Soc., Dalton Trans.*, 1990, 677.

11 D. A. T. Young, R. J. Wiersema and M. F. Hawthorne, *J. Am. Chem. Soc.*, 1971, **93**, 5687; M. R. Churchill and A. H. Reis, *J. Chem. Soc., Dalton Trans.*, 1972, 1314.

12 (*a*) J. A. Doi, R. G. Teller and M. F. Hawthorne, *J. Chem. Soc., Chem. Commun.*, 1980, 80; (*b*) J. A. Long, T. B. Marder, P. E. Behnken and M. F. Hawthorne, *J. Am. Chem. Soc.*, 1984, **106**, 2979; (*c*) C. B. Knobler, T. B. Marder, E. A. Mizusawa, R. G. Teller, J. A. Long, P. E. Behnken and M. F. Hawthorne, *J. Am. Chem. Soc.*, 1984, **106**, 2990.

13 F.-E. Baumann, J. A. K. Howard, O. Johnson and F. G. A. Stone, *J. Chem. Soc., Dalton Trans.*, 1987, 2661; D. D. Devore, C. Emmerich, J. A. K. Howard and F. G. A. Stone, *J. Chem. Soc., Dalton Trans.*, 1989, 799.

14 G. M. Sheldrick, SHELXTL PLUS programs for use with the Siemens R3m/V X-ray system.

Received 28*th October* 1991; *Paper* 1/05463E